

# Hyper Parameters Optimization for Effective Brain Tumor Segmentation with YOLO Deep Learning

R. Anita Jasmine<sup>1</sup>, P. Arockia Jansi Rani<sup>2</sup>, J. Ashley Dhas<sup>3</sup>

<sup>1</sup>Assistant Professor, SRM Institute of Science and Technology, Chennai, India

<sup>2</sup>Associate Professor, Department of Computer Science and Engineering, Manonmaniam Sundaranar University, Tirunelveli, India

<sup>3</sup>Assistant Professor, C.S.I Institute of Technology, Thovalai, India

Email: anitajar@srmist.edu.in

DOI: 10.47750/pnr.2022.13.S06.292

## Abstract

In the field of neuroimaging, differential diagnosis of brain tumour primarily relies on the visual appearance of the tumor in the MRI. For better analysis of brain tumours segmentation of tumour ROI is indispensable. The objective of this work is to develop a deep network for brain tumour segmentation using YOLO with TIC+ High grade and FLAIR low grade tumour images from the BRATS dataset. As the hyper parameters play a crucial role in the efficacy of the CNN, an exhaustive search is made to arrive at the optimal hyper parameters. The number of anchor boxes, mini batch size and the learning algorithm are carefully evaluated to arrive at the optimal values. The visual analysis of segmentation proves the effectiveness with 4 anchor boxes, mini batch size 16 and Adam optimizer. The mean average precision value of 0.9688 and recall value of 0.9841 is obtained for HGG segmentation. The mean average precision value as 0.8435 and recall value of 0.8552 is obtained for LGG segmentation. The accuracy of the tumor detector computed with Mean IoU score is 100% for HGG and 98% for LGG tumor images. The tumor image segmented using YOLO is further subjected to histogram and region growing techniques to segment the ring and lesion core of the brain tumor which may be used for further analysis of benign and malignant tumor. As YOLO CNN could fix the bounding box with highest accuracy, the traditional skull stripping pre-processing techniques can be skipped for tumor segmentation.

**Keywords:** Low Grade Glioma, High Grade Glioma, YOLO CNN, Deep Learning, TIC+ and FLAIR MRI.

## 1. INTRODUCTION

Tumor ROI segmentation plays an important role in tumor classification as it eliminates the interference of non-tumor tissues in diagnosis. Deep learning networks have proven its efficacy over conventional segmentation techniques. YOLO (You Look Only Once) the CNN designed for real time object detection, is adopted for tumor bounding box location in two different brain tumor datasets. The strength of these deep neural networks are its hyper-parameters and arriving at the optimized set of hyper parameters is a big challenge. The best configured CNN promises highest accuracy in classification. The heuristic is to experimentally analyze the impact of hyper parameters in the accuracy with extensive trial and error approach. The objective of this paper is to find the optimal hyper parameters for the YOLO network to achieve maximum accuracy for tumor ROI segmentation. The role of hyper parameters are explained, the experimental results for different values of hyper parameters are discussed and the optimal parameters are tabulated.

## 2. Related Works

Deep learning algorithms outperform the conventional segmentation algorithms as they automatically extract features from images with vast computation on image as a whole. These features has proven well than the handcrafted features [1]. Recently in BRATS tumor segmentation challenge these CNN has ranked top than the other techniques [2] [3]. Region proposal methods such as R-CNN [4], Fast R-CNN [5], and Faster R-CNN [6] mainly rely on texture, edge, color intensity information in the image for segmentation. In spite of its better performance, it did not fit well for real time object detection. As the network goes



Visualization of the labelled bounding boxes in the training data helps to understand the range of bounding boxes and to select the number and shape of bounding box for training the network. Intersection over Union (IoU) metric which is invariant to size is used to identify the optimal number of bounding boxes and is given by the Equation (4.1) .

$$IoU(b1,b2)=\frac{\min(w1,w2)*\min(h1,h2)}{(w1h1+w2h2)-\min(w1,w2)*\min(h1,h2)} \quad (1)$$

Where w1, h1, w2, h2 are the widths and heights of bounding boxes b1 and b2.

Initially based on visual analysis of the box area versus aspect ratio a rough estimate for the number of anchor boxes is chosen. The k-means algorithm with IoU distance metric is computed to cluster the bounding boxes. The number of clusters is equal to the number of anchor boxes. The mean IoU value greater than 0.5 indicates the best overlap of the anchor boxes with the bounding boxes in the training data.

### 3.2 Training Options

The hyper parameters focused to improve the segmentation results in this research are the mini batch size and learning algorithm for error optimization.

### 3.3 Mini Batch Size

Gradient descent Algorithm is used to find the coefficients to minimize the error of the network. The coefficients are adjusted such that the slope of errors are moved to a minimum. Mini Batch gradient descent Algorithm takes in the advantage of robustness of stochastic gradient descent and the efficiency of Batch gradient descent Algorithm. It groups the training data based on the batch size, evaluates the samples in the group and updates the model for minimizing the error. The batch sizes are modelled as power of 2 so as to fit the memory requirements of the CPU hardware. For smaller batch size values, the convergence is quick but the noise inducement is high. For larger batch size values, the convergence is slow but the noise inducement is less. The batch size selection is also considered based on the number of images in the training data and the frequency of similar objects in the training data. In this research, the performance is evaluated with mini batch sizes of 4, 16 and 32. The visual and quantitative results are discussed in the following section.

### 3.4 Learning Algorithm

As one more step to improve the accuracy, the optimal batch size derived from Batch gradient descent Algorithm is tested with Adam optimizer algorithm. The speed of convergence is more when compared to the gradient descent Algorithm due to the momentum term calculation to achieve fast convergence. The adaptive learning rate feature improves the accuracy of the trained model.

### 3.5 Object Detection Using YOLO

YOLO divides the input image into S X S non overlapping grid cells. A weighted feature set is computed for each grid cell. From the feature set value, a probability is associated with each grid cell for each bounding box. The predictions are denoted by (S X S) \* B \*(5+C) tensor. Where B is the bounding box and C denotes the number of classes. The metrics used for YOLO performance evaluation are mAP and IOU. IOU implies the accuracy of the object detection and is given by the Equation (2),

$$IOU=\frac{\text{Area of Overlap of ground truth and predicted bounding box}}{\text{Area of Union of ground truth predicted bounding box}} \quad (2)$$

The mean Average Precision (mAP) compares the similarity of the predicted and ground truth bounding box and returns a score. The higher score value indicates the higher accuracy in detection. For precision p and recall r the mAP is given by the Equation (3),

$$mAP=\frac{1}{N}\sum_{r=0}^1(\max(p(r')) \text{ such that } r' \geq r) \quad (3)$$

## 4. EXPERIMENTAL SETUP

This experimental study is carried with the BRATS dataset for high grade and low grade glioma segmentation and REL dataset. The model developed for HGG segmentation is adopted to locate the tumor in the REL dataset.

### 4.1 BRATS Dataset

As the two different tumor types HGG and LGG vary in their visual appearance, separate model is developed for accurate segmentation. The T1 C+ MRI captures significant details for high grade glioma classification with the high intense ring surrounding the low intense tumor core which in turn encircled with the edema. Similarly for low grade glioma, FLAIR images highlights the bright ring surrounding the less intense tumor core and so 700 T1C+ and FLAIR images for used in this research for brain tumor segmentation

### 4.2 REL Dataset

This dataset comprises of 242 T1 weighted MRI with abscess, metastasis, glioma and meningioma. The images are collected from SP Scans, Nagercoil and downloaded from Raediopedia. The dataset is divided into two classes, benign (80 images) and malignant (162 images).

Table 1 Anchor Boxes and IoU for the Tumor images

Tumor	Count	Anchor box values	Mean IoU
HGG	4	[51 45; 44 36; 63 57; 33 31]	0.828
	5	[51 45; 49 34; 40 37; 63 57; 31 29]	0.841
	6	[40 37; 31 29; 49 34; 64 57; 49 50; 52 43]	0.853
LGG	4	[43 37; 59 37; 89 70; 79 54]	0.814
	5	[43 37; 59 37; 89 70; 75 51; 79 54]	0.838
	6	[88 59; 47 42; 94 76; 69 50; 42 31; 57 47]	0.845

### 4.3 Training and Testing Data

For training the model 550 images in each tumor type are labeled using Matlab Image Labeler. The aspect ratio of the bounding boxes in each training image is evaluated for anchor box estimation. The model is trained with different batch size and learning algorithm. 150 images of each tumor type is used for testing the model.

## 5. RESULTS

The YOLO models are developed for brain tumor segmentation after an in-depth research of three different parameters. Figure 2 and Figure 3 show the plot of anchor boxes for HGG and LGG images. Table 1 shows the anchor box values and the mean IoU values.

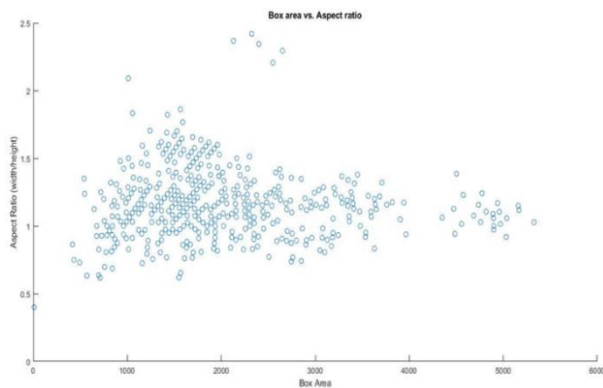


Figure 2 Anchor Box estimation with box area and aspect ratio for HGG tumors

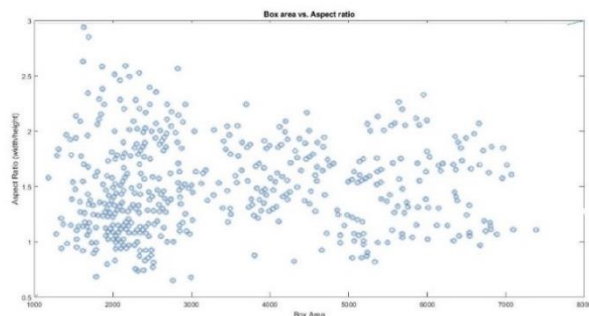


Figure 3 Anchor Box estimation with box area and aspect ratio for LGG tumors

Table 2 through Table 4 shows the training loss values for the three different mini batch sizes with base Learning rate=0.001. The table values prove the performance of the model with the batch size 16. The fluctuation of the mini batch loss values indicates the dynamics of the trained model. To arrive at a stable model the loss should be stable. With this mini batch size the results are further pruned with adam optimizer learning algorithm. Figure 4 shows the visual performance of the model with the HGG and LGG tumor in the test data.

Table 2 Training Results for mini batch size 4

Epoch	Iteration	Time Elapsed	Mini-batch	Error Gradient
		(hh:mm:ss)	RMSE	(Mini-batch loss)
1	1	00:00:07	7.9	62.5
1	50	00:04:01	2.81	7.9
2	100	00:07:47	3.41	11.6
3	150	00:11:37	0.93	0.9
4	200	00:15:25	1.07	1.1
5	250	00:19:10	0.64	0.4
6	300	00:22:55	0.77	0.6
7	350	00:26:40	0.81	0.7
8	400	00:30:25	0.62	0.4
9	450	00:34:09	0.42	0.2
9	500	00:37:52	0.49	0.2
10	550	00:41:37	0.5	0.3

Table 3 Training Results for mini batch size 32

Epoch	Iteration	Time Elapsed (hh:mm:ss)	Mini-batch RMSE	Error Gradient (Mini-batch loss)
1	1	00:02:02	6.9	47.6
4	50	00:30:16	3.6	12.9
7	100	00:55:18	3.84	14.8
10	150	01:19:53	3.9	15.2
10	160	01:24:46	4.06	16.4

Table 4 Training Results for mini batch size 16

Epoch	Iteration	Time Elapsed (hh:mm:ss)	Mini-batch RMSE	Mini-batch Loss
1	1	00:00:21	6.9	47.6
2	50	00:14:42	0.65	0.4
4	100	00:29:14	0.41	0.2
5	150	00:42:56	0.47	0.2
7	200	00:56:37	0.38	0.1
8	250	01:10:44	0.31	0.94
10	300	01:24:39	0.35	0.1
10	320	01:29:42	0.35	0.1

The trained model for segmentation with the optimal parameters is tested against the test data in REL dataset and BRATS dataset. The visual performance is instanced in the Figure 5. In case of more than one bounding box computed, the one with maximum IoU score value is picked up using Non Max suppression technique. The predicted bounding boxes with IoU score greater than 0.5 is considered as the valid one.

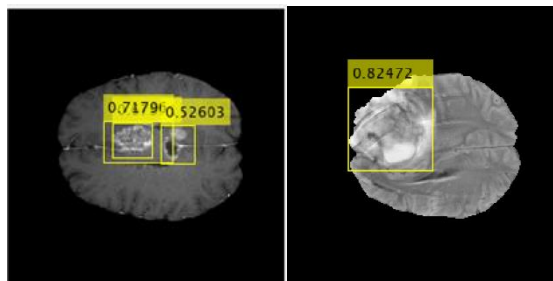


Figure 4 Visual Analysis of HGG and LGG segmentation using YOLO

The trained model for segmentation with the optimal parameters is tested against the test data in REL dataset and BRATS dataset. The visual performance is instanced in the Figure 5. In case of more than one bounding box computed, the one with maximum IoU score value is picked up using Non Max suppression technique. The predicted bounding boxes with IoU score greater than 0.5 is considered as the valid one.

## 6. Discussion and Conclusion

Hyper parameter optimization is crucial for Deep learning networks. In this research work three different parameters which has an active influence in the segmentation is evaluated and the best optimum values are formulated. In the case of anchor box optimization different count values from 4 through 6 is experimented. The plot of Number of Anchors versus Mean IoU is illustrated in Figure 6.

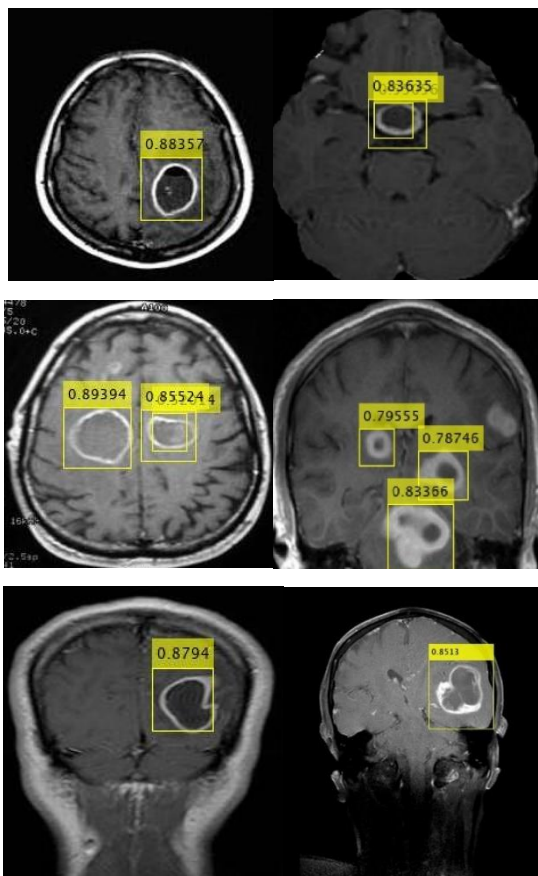


Figure 5 Visual Analysis of REL segmentation using YOLO with skull MRI

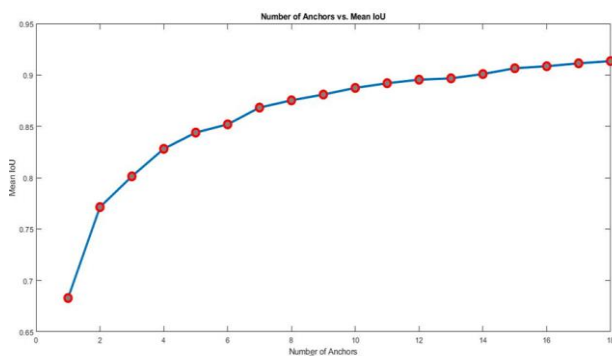


Figure 6 Number of Anchors versus Mean IoU

Though the mean IoU values gradually increases with the count of anchor boxes, the aspect ratio values of the bounding boxes did not show significant variation. The mean IoU value for anchor box count 4 is greater than 0.8. As the speed of the prediction decreases with increase in the number of anchor boxes, the method is tested with 4 anchor boxes and the final results in segmentation proves this to be the suitable choice. Figure 7 through 9 illustrates the plot of Training Loss for batch sizes 4, 16 and 32. From the inference on these figures, batch size 16 proves to be optimal for the model.

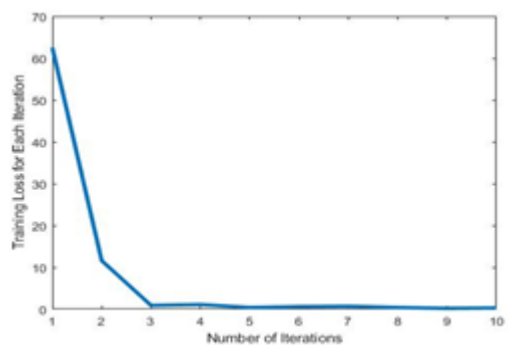


Figure 7 Training Loss for batch size 4

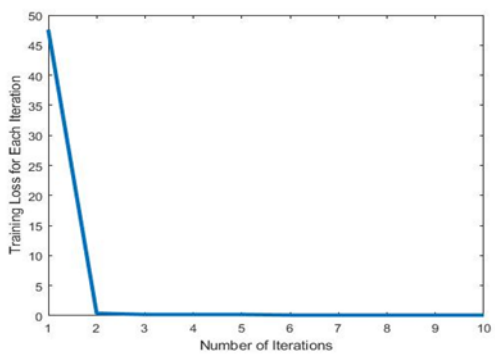


Figure 8 Training Loss for batch size 16

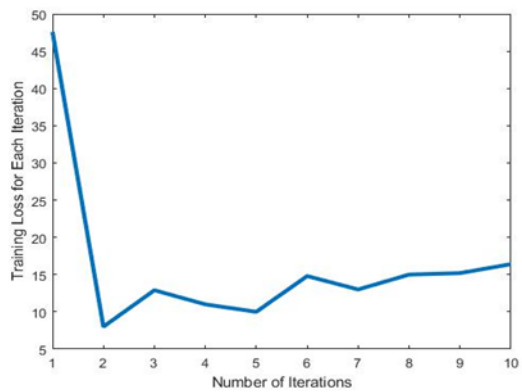


Figure 9 Training Loss for batch size 32

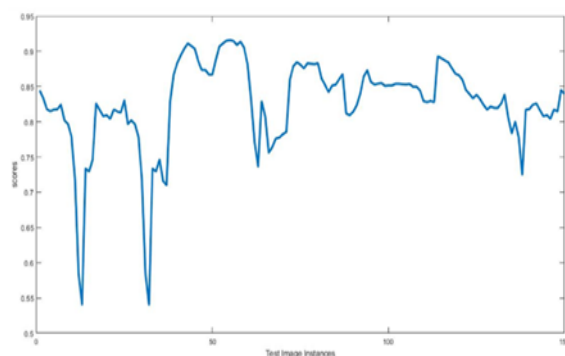


Figure 10 Plot of scores obtained using bounding box overlap ratio for HGG images

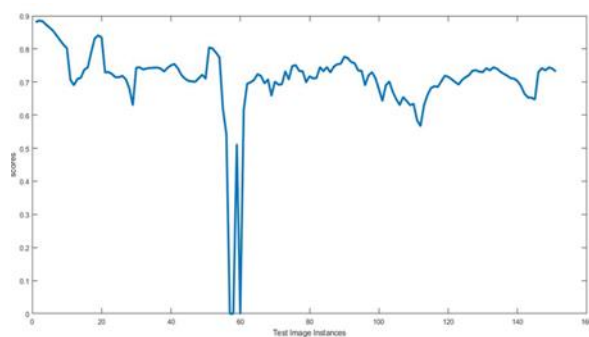
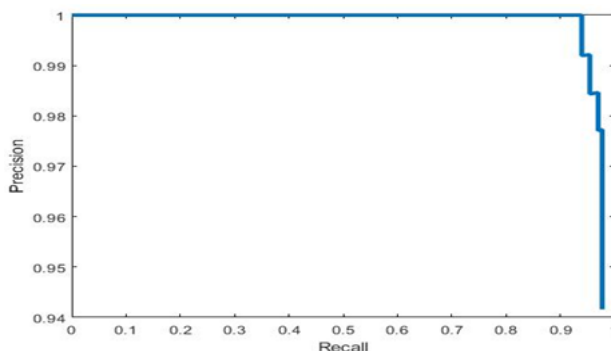


Figure11 Plot of scores obtained using bounding box overlap ratio for LGG Images



Mini Batch Size is the fixed number of training samples less than the training data used for training the CNN with small dataset. The mini batch size should be fixed such that the error is minimum for the training data. And regarding the mini batch size for error approximation, 16 performs well which is obvious in Figure 8. Actually mini batch size 32 is suggested for better performance, but this value experimentally yielded poor performance as indicated in Figure 9.

This is because of the varying size of brain tumors. Mini Batch size 16 resulted in better performance than mini batch 4. With this batch size the performance is analyzed with two different algorithm for error approximation. Adam optimizer improved the results of stochastic gradient descent algorithm minimizing the error. The segmentation results with 4 anchor boxes, mini batch size 16 and adam optimizer proves to be the optimal hyper parameter values for brain tumor segmentation. A predicted bounding box is valid if it would overlap with the ground truth bounding box by more than 50%.

The score values lies in the range of 0 and 1 and increases with the increase of the area of overlap between the ground truth and predicted bounding box. Figure 10 illustrates plot of bounding box overlap scores for HGG images. The graph shows the scores for all the test images is greater than 0.5 which indicates the efficiency of fixing the bounding box around the brain tumor.

Figure 11 illustrates the plot of bounding box overlap ratio scores for LGG images. Except for two samples in the test dataset the model works good for fixing the bounding boxes. The precision recall curve implies the trade-off between precision and recall values. This curve helps to fix the critical point with higher precision and zrecall values. Figure 12 and 13 illustrates the precision recall value for HGG and LGG test images. Figure 12 indicates the mean average precision value as 0.9688 and recall value of 0.9841 for HGG images. Figure 13 indicates the mean average precision value as 0.8435 and recall value of 0.8552 for LGG images. The performance of the method when evaluated with Bounding Box Overlap ratio yielded 99.5% accuracy for HGG, 98% for LGG and 97% accuracy for REL tumor segmentation. The trained model is used to segment BRATS tumor images and REL dataset. The HGG TIC+ MRI from BRATS 2013 dataset is segmented using the trained model and histogram and region growing techniques discussed in the chapter 3. The proposed method is compared with the state-of-art methods and illustrated in Table 5.

Table 5 Comparison of the brain tumor segmentation methods using Dice Scores (Results obtained using BRATS 2013 Dataset)

Authors	Whole Tumor	Core Tumor	Enhancing Tumor
Havaei et al., [10]	0.86	0.77	0.73
Hamamci et al., [11]	0.72	0.57	0.59
Kwon et al., [12]	0.88	0.83	0.72
Tustison et al., [13]	0.87	0.78	0.74
Havaei et al., [14]	0.88	0.79	0.73
Pereira et al., [15]	0.88	0.79	0.73
Zhao, et al., [16]	0.81	0.90	0.75
Proposed work	0.89	0.90	0.92

For glioma segmentation this method performs better than SVM and Fuzzy c-means classification. In this proposed method, the combination of YOLO CNN with histogram and region growing techniques gives a better performance when compared with other techniques. There is no need of skull stripping of the input brain MRI as the YOLO is trained with predefined bounding boxes. The segmented tumor ROI using YOLO is further segmented into ring and lesion core using histogram and region growing techniques and the results are compared with the state of art techniques tabulated in Table 5. The results highlights the performance of the method. The Dice score values for segmentation of the whole tumor is 0.89, the tumor core is 0.90 and the enhancing region is 0.92. From this search of optimal hyper parameters the segmentation results are refined which could definitely increase the accuracy for tumor diagnosis and treatment. The future works aim to optimize the hyper parameters for volumetric brain tumor segmentation using CNN.

## REFERENCES

- [1] Pereira, S., Pinto, A., Alves, V., Silva, C.A.: Brain Tumor Segmentation using Convolutional Neural Networks in MRI Images. *IEEE Trans. Med. Imaging*. 35, 1240–1251 (2016).
- [2] Havaei, M., Davy, A., Warde-Farley, D., Biard, A., Courville, A., Bengio, Y., Pal, C., Jodoin, P.-M., Larochelle, H.: Brain tumor segmentation with Deep Neural Networks. *Med. Image Anal.* 35, 18–31 (2016).
- [3] Kamnitsas, K., Ledig, C., Newcombe, V.F.J., Simpson, J.P., Kane, A.D., Menon, D.K., Rueckert, D., Glocker, B.: Efficient multi-scale 3D CNN with fully connected CRF for accurate brain lesion segmentation. *Med. Image Anal.* 36, 61–78 (2017).
- [4] Girshick, R.; Donahue, J.; Darrell, T.; Malik, J. Rich feature hierarchies for accurate object detection and semantic segmentation. In *Proceedings of the 2014 IEEE Conference on Computer Vision and Pattern Recognition*, Washington, DC, USA, 23–28 June 2014; pp. 580–587.
- [5] Girshick, R. Fast R-CNN. In *Proceedings of the 2015 IEEE International Conference on Computer Vision*, Santiago, Chile, 7–13 December 2015; pp. 1440–1448
- [6] Ren, S.Q.; He, K.M.; Girshick, R.; Sun, J. Faster R-CNN: Towards Real-Time Object Detection with Region Proposal Networks. *IEEE Trans. Pattern Anal.* 2017, 39, 1137–1149.
- [7] Redmon, J.; Farhadi, A. YOLO9000: Better, Faster, Stronger. In *Proceedings of the 2017 IEEE Conference on Computer Vision and Pattern Recognition Workshops*, Honolulu, HI, USA, 21–26 July 2017; pp. 6517–6525.
- [8] Redmon, J.; Farhadi, A. YOLOv3: An incremental improvement. *arXiv* 2018, arXiv:1804.02767.
- [9] Redmon, J.; Divvala, S.; Girshick, R.; Farhadi, A. You Only Look Once: Unified, Real-Time Object Detection. In *Proceedings of the 2016 IEEE Conference on Computer Vision and Pattern Recognition*, Las Vegas, NV, USA, 27–30 June 2016; pp. 779–788.
- [10] Havaei M, Larochelle H, Poulin P, Jodoin P M. Within-brain classification for brain tumor segmentation. *Int J Cars* 2016; 11:777-788
- [11] Hamamci A, et al. Tumor-Cut: segmentation of brain tumors on contrast enhanced MR images for radiosurgery applications. *IEEE Trans Med Imaging* 2012; 31(3):790–804.

- [12] D. Kwon et al. Combining generative models for multifocal glioma segmentation and registration. *Medical Image Computing and Computer-Assisted Intervention–MICCAI 2014*. Springer, 2014:763–770.
- [13] Tustison N. et al. Optimal symmetric multimodal templates and concatenated random forests for supervised brain tumor segmentation (simplified) with ants. *Neuroinformatics* 2015;13(2): 209–225.
- [14] Havaei, M. , Davy, A. , Warde-Farley, D. , Biard, A. , Courville, A. , Bengio, Y. , et al. , 2017. Brain tumor segmentation with deep neural networks. *Med. Image Anal.* 35, 18–31 .
- [15] Pereira, S. , Pinto, A. , Alves, V. , Silva, C.A. , 2016. Brain tumor segmentation using convolutional neural networks in MRI images. *IEEE Trans Med. Imaging* 35, 1240–1251 .
- [16] Zhao, X. , Wu, Y. , Song, G. , Li, Z. , Fan, Y. , Zhang, Y. , 2016. Brain tumor segmentation using a fully convolutional neural network with conditional random fields. In: *International Workshop on Brainlesion: Glioma, Multiple Sclerosis, Stroke and Traumatic Brain Injuries*, pp. 75–87 .